DOI: 10.23968/2500-0055-2025-10-2-88-96

# PLASTIC BUCKLING ANALYSIS OF CONVENTIONAL CONCRETE AND EXPANDED POLYSTYRENE CONCRETE SPHERICAL SHELLS

Issaias Anday Sereke*, Marina Igorevna Rynkovskaya, Habte Yohannes Damir

Peoples' Friendship University of Russia named after Patrice Lumumba (RUDN University), Moscow, Russia

*Corresponding author's email: issaiasanday@gmail.com

**Abstract**

**Introduction**: Concrete's self-weight is the primary factor contributing to increased cross-sectional dimensions and dead loads in structures. This disadvantage can be mitigated by using suitable lightweight concrete. Expanded polystyrene concrete (EPSC), which is lighter than conventional concrete, has not yet been implemented in shell structures. The **purpose of the study** was to analyze and compare the plastic buckling capacities of conventional concrete and EPSC domes, and to develop an analytical formula for determining the plastic buckling capacity of spherical shells made from these materials. The **methodology** includes an experimental investigation involving cube test specimens to evaluate the properties of EPSC. Based on the test results, the compressive strength, density, and elastic modulus of EPSC were found to be 9.48 MPa, 2074.17 kg/m$^3$, and 11.18 GPa, respectively. Subsequently, linear buckling analysis (LBA) and material non-linear analysis (MNA) were performed using ABAQUS to determine the elastic and plastic buckling resistances of 36 concrete and 36 EPSC spherical shells. Based on the analysis results, an analytical formula was developed to estimate the plastic buckling capacities of both concrete and EPSC shells. **Results**: The findings reveal that the plastic buckling resistance of EPSC shells is significantly higher than practically applied external uniform pressures. However, the plastic buckling resistance of EPSC shells is lower than that of equivalent concrete shells. Despite this, EPSC shells exhibit lower plastic deformations and displacements compared to their concrete counterparts, indicating sufficient stiffness of such shells and supporting EPSC use in spherical shell construction. The proposed formula can be easily applied to determine the reference plastic buckling capacities of concrete and EPSC spherical shells.

**Keywords:** buckling; pressure; concrete; displacement; spherical shells.

## Introduction

The phenomenon of plastic buckling in shells was first demonstrated through the behavior of a moderately thick cylindrical shell, which exhibited both axisymmetric and non-axisymmetric deformations under axial compression. It was observed that, at the peak of the load–deflection curve, the modes of failure involved in plastic buckling included bifurcation buckling and non-linear collapse, as illustrated in Fig. 1.

As seen in Fig. 1a, between points O and A lies the bifurcation point B. A structure will begin to fail through rapidly increasing non-axisymmetric deformations if axisymmetric deformation follows the path OAC and non-axisymmetric deformation follows the path BD. In such a case, at the load level $\lambda_L$, bifurcation buckling becomes more critical than non-linear collapse (Bushnell, 1982). However, in real geometrically imperfect shell structures, bifurcation buckling does not occur. Instead, these structures typically exhibit snap-through failure at point E along the path OEF, corresponding to the collapse load $\lambda_s$.

Several studies have investigated the stability behavior of spherical shells under external pressure. The first analytical solution for the elastic buckling of perfect spherical shells was derived by Zoelly (1915). Later works focused on the post-buckling behavior of spherical shells under external pressure (Budiansky and Hutchinson, 1966; Sato et al., 2012; Hutchinson, 2016), and on the axisymmetric buckling of spherical shells filled with an elastic medium under external pressure (Sato et al., 2012). Nevertheless, studies on the plastic buckling of spherical shells under external pressure remain relatively scarce compared to studies on elastic buckling. In general, plastic buckling research has predominantly focused on circular cylindrical shells subjected to axial compression (Do et al., 2023). In this context, the present study focuses on the plastic buckling of spherical concrete shells made from lightweight material.

While conventional concrete used in spherical shells is known for its durability and flexibility, its high self-weight significantly increases the structural dead load and necessitates a larger cross-section. For effective shell design, optimizing construction materials is essential. One promising approach is to produce lightweight concrete by partially or fully substituting natural stone aggregates or sand with alternative lightweight aggregates (Srinivas et al., 2021). In this regard, expanded polystyrene (EPS) has been employed to partially replace concrete aggregates and sand, resulting in lightweight expanded polystyrene concrete (EPSC) (Damir et al., 2024).

As mentioned earlier, the dead load due to concrete self-weight constitutes a major portion



**For citations:** Sereke, I. A., Rynkovskaya, M. I., Damir, H. Y. (2025). Plastic buckling analysis of conventional concrete and expanded polystyrene concrete spherical shells. Architecture and Engineering, No 2 (10), pp. 88–96. DOI: 10.23968/2500-0055-2025-10-2-88-96.

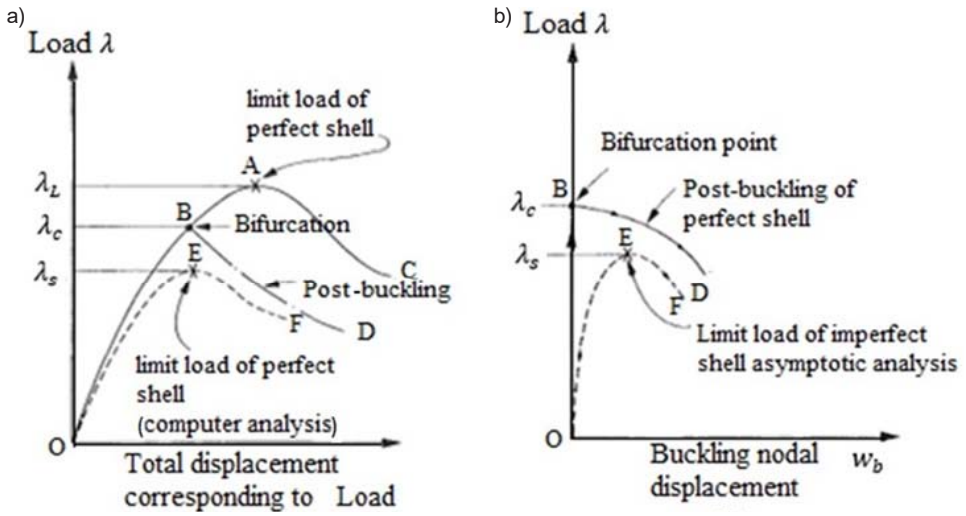


Fig. 1. Load–displacement curves indicating bifurcation and limit points (Bushnell, 1982)

of the total structural load, leading to increased cross-sections and higher construction costs. This research is motivated by the lower weight and cost advantages of EPSC over conventional concrete, the lack of studies on EPSC spherical shells, and the limited existing research on the plastic buckling of spherical shells. This paper aims to:

• Study the properties of EPSC, including density, compressive strength, and modulus of elasticity.

• Analyze the plastic buckling behavior and associated displacements of EPSC spherical shells in comparison to equivalent conventional concrete shells through numerical modeling in ABAQUS.

• Finally, develop an analytical formula to determine the plastic buckling capacity of both concrete and EPSC spherical shells.

**Materials and Methods**

The materials used in the current study are ordinary concrete and expanded polystyrene concrete (EPSC). Ordinary concrete typically has a density range of 2200–2600 kg/m$^3$, whereas the density of EPSC can vary from 800 to 2000 kg/m$^3$, depending on the percentage of EPS beads used (Liu and Chen, 2014; Saradhi Babu et al., 2005; Zia et al., 1997). When lightweight EPSC is used instead of ordinary concrete, the effects of inertia and seismic forces can be significantly reduced (Aghaee and Foroughi, 2013; Akçaözoğlu et al., 2010; Yasin et al., 2016; Maghfouri et al., 2020; Teo et al., 2006).

As with any material, the mechanical properties of EPSC must be thoroughly studied before it can be recommended for structural or non-structural applications. EPSC has already been used in various applications such as cladding panels, curtain walls, composite flooring systems, load-bearing blocks, and pavements (Sri Ravindrarajah and Tuck, 1994). However, to date, it has not been applied in shell structures. Before investigating the plastic buckling behavior of EPSC spherical shells, a laboratory study was conducted to evaluate the properties of the EPSC mix.

In this study, a volumetric mix proportion of 1:2:3 for cement, sand, and coarse aggregate was used. EPS was used to replace 33.33 % of the coarse aggregate and 16.67 % of the sand. The ingredients were mixed in a specific sequence using a mixer, with a water-to-cement (w/c) ratio of 0.6. First, the dry EPS beads were combined with a portion of the water to allow the beads to become wetted. Then, the remaining ingredients were gradually added along with the rest of the water until a uniform, flowable mix was achieved. The mix proportions are summarized in Table 1.

Three cube specimens, each measuring 150 × 150 × 150 mm, were prepared for laboratory testing. The mix was poured into the molds in three layers, with hand compaction applied after each layer. The top surface of each specimen was leveled using a trowel. After 24 hours, the specimens were demolded and covered with a damp cloth for three days. The weight, density, and compressive strength of the specimens were measured at 28 days, as shown in Fig 2.

Table 2 presents the laboratory results for the three EPSC cube specimens. Based on these results, the average compressive strength and density were calculated to be 9.48 MPa and 2074.17 kg/m$^3$, respectively.

The elastic modulus of EPSC was calculated based on the ACI 318-19 (ACI Committee, 2019)

Table 1. **EPSC Mix Proportion**

| Cement : Sand : Aggregate | % of Sand Replaced by EPS | % of Coarse Aggregate Replaced by EPS | W/C Ratio |
|---|---|---|---|
| 1 : 2 : 3 | 16.67 | 33.33 | 0.6 |

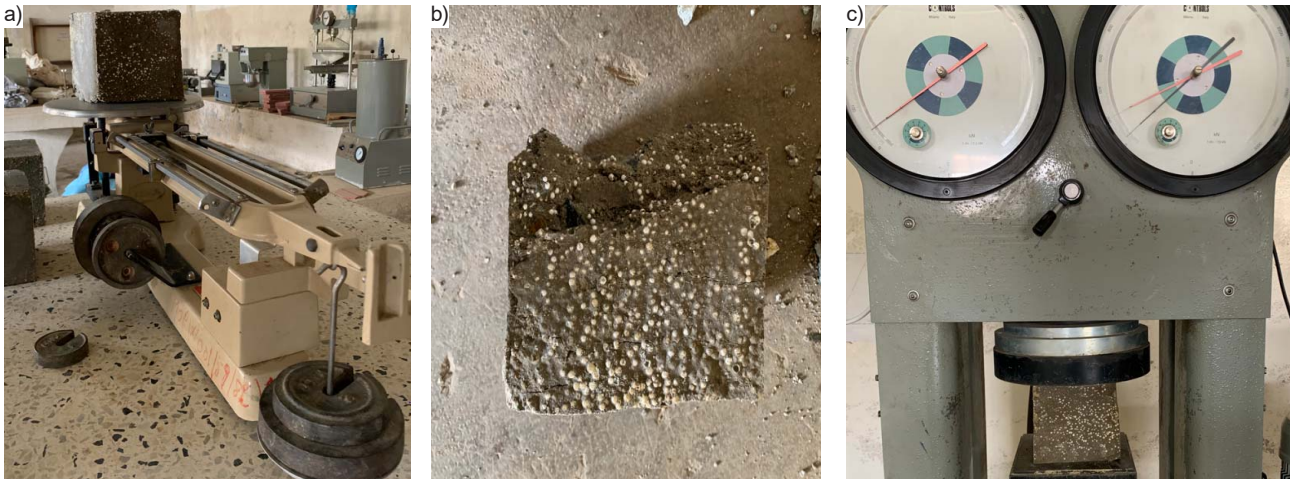


Fig. 2. Sample measurements: a — EPSC cube specimen on a weighing balance; b — Crushed EPSC cube specimen c) EPSC cube specimen tested for compressive strength

metric equation (1) for lightweight concrete with density $w_c$ ranging from 1,404 to 2,560 kg/m$^3$:

$$E_c = w_c^{1.5} \cdot 0.043 \cdot \sqrt{f'_c}, \quad (1)$$

where: $E_c$ — static elastic modulus in MPa;

$w_c$ — concrete density in kg/m$^3$;

$f'_c$ — cylinder compressive strength of concrete in MPa.

To convert cube compressive strength to equivalent cylinder strength, the following equation was used (Akter et al., 2017):

Cylinder strength = 0.8 x cube strength. (2)

Using Eqs. (1) and (2), the modulus of elasticity and cylinder compressive strength were calculated as 11.18 GPa and 7.58 MPa, respectively. The Poisson's ratio of EPSC was taken as 0.22, consistent with values for other low-strength concretes (Neville, 2012).

For the analysis of concrete and EPSC spherical shells, the following material properties were used:

Concrete (C20):

- Cylinder compressive strength: 20 MPa;
- Unit weight: ($\gamma_c = 24$ kN/m$^3$);
- Modulus of elasticity: $E_c = 22.61$ GPa;
- Poisson's ratio: $\upsilon = 0.2$.

EPSC:

- Cylinder compressive strength: 7.58 MPa;
- Unit weight: ($\gamma_{EPSC} = 20.74$ kN/m$^3$);
- Modulus of elasticity: $E_{EPSC} = 11.18$ GPa;
- Poisson's ratio: $\upsilon = 0.22$.

After establishing the properties of EPSC, 36 linear buckling analyses (LBA) and 36 material non-linear analyses (MNA) were performed on 36 spherical shell models made of both concrete and EPSC. These shells had half-opening angles Ø ranging from 20° to 90°, and the analyses were conducted using ABAQUS. Shell thicknesses were chosen as 70 mm, 73.68 mm, 77.77 mm, 82.35 mm, 87.5 mm, and 93.33 mm, corresponding to *R*/*t* ratios of 100, 95, 90, 85, 80, and 75, respectively. All shells shared a constant radius of curvature of 7,000 mm. The shell models were subjected to fixed boundary conditions, which are widely adopted in engineering applications (Liu et al., 2022; Wang et al., 2019). In each analysis, the shells were subjected to external pressure acting normal to their surfaces (Muc et al., 2022; Zhang et al., 2017). The geometric configuration of the shell models is shown in Fig. 3.

During the material non-linear analysis (MNA), each shell was loaded using its corresponding first eigenvalue load obtained from the linear buckling analysis (LBA). To develop the analytical formula for determining the plastic buckling capacity ($PR_{pl}$) of concrete and EPSC spherical shells, the MNA method — based on perfect shell bending theory — was employed (Rotter and Schmidt, 2013). This approach aligns with guidelines in Eurocode 3 (European Committee for Standardization, 2007) and findings by Abood (2020) and Błażejewski (2022).

**Results and Discussion**

The results for the 36 elastic and plastic buckling pressures ($PR_{pl}$) of conventional concrete shells, obtained from LBA and MNA respectively, are summarized in Tables 3 and 4.

Graphs of the plastic buckling capacities ($PR_{pl}$) obtained from ABAQUS software analysis, plotted against the R/t ratios of the 36 concrete shells,

Table 2. **Laboratory Results for the EPSC Cube Specimens**

| Test Specimen No. | Mass (kg) | Density (kg/m$^3$) | Force (kN) | Compressive Strength (MPa) |
|---|---|---|---|---|
| 1 | 7.155 | 2,120 | 235 | 10.44 |
| 2 | 6.948 | 2,058.66 | 207 | 9.2 |
| 3 | 6.898 | 2,043.85 | 198 | 8.8 |

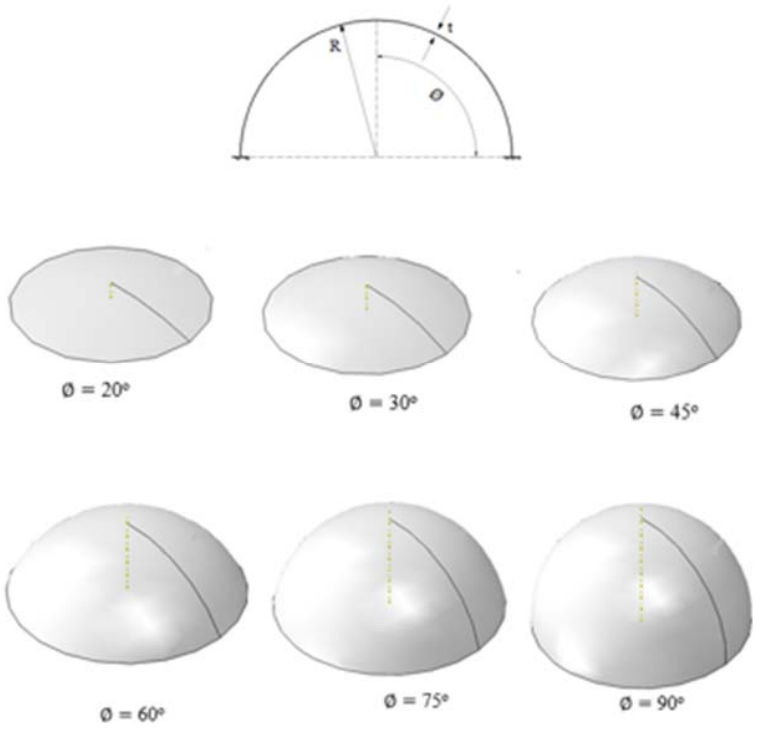


Fig. 3. Geometric configuration of the shell models

Table 3. **Elastic Critical Buckling Pressures ($PR_{cr}$) of Concrete Shells**

| Geometric Dimensions of the Shells | | | Critical Pressures for the Shells with Varying Half-Angle Ø (MPa) | | | | | |
|---|---|---|---|---|---|---|---|---|
| *R* (mm) | *t* (mm) | *R*/*t* | 20° | 30° | 45° | 60° | 75° | 90° |
| 7,000 | 70 | 100 | 2.8630 | 2.7726 | 2.7104 | 2.6846 | 2.6685 | 2.6677 |
| 7,000 | 73.68 | 95 | 3.1697 | 3.0802 | 3.0073 | 2.9723 | 2.9528 | 2.9528 |
| 7,000 | 77.77 | 90 | 3.5342 | 3.4372 | 3.3510 | 3.3136 | 3.2929 | 3.2913 |
| 7,000 | 82.35 | 85 | 3.9744 | 3.8553 | 3.7623 | 3.7182 | 3.6900 | 3.6876 |
| 7,000 | 87.5 | 80 | 4.5133 | 4.3599 | 4.2544 | 4.1975 | 4.1692 | 4.1654 |
| 7,000 | 93.33 | 75 | 5.1838 | 4.9773 | 4.8442 | 4.7843 | 4.7542 | 4.7346 |

Table 4. **Plastic Buckling Pressures ($PR_{pl}$) (MPa) of Concrete Shells**

| Geometric Dimensions of the Shells | | | Plastic Buckling Pressures for the Shells with Varying Ø | | | | | |
|---|---|---|---|---|---|---|---|---|
| *R* (mm) | *t* (mm) | *R*/*t* | 20° | 30° | 45° | 60° | 75° | 90° |
| 7,000 | 70 | 100 | 0.4066 | 0.4019 | 0.4004 | 0.4001 | 0.4000 | 0.4000 |
| 7,000 | 73.68 | 95 | 0.4285 | 0.4231 | 0.4215 | 0.4210 | 0.4210 | 0.4210 |
| 7,000 | 77.77 | 90 | 0.4529 | 0.4469 | 0.4448 | 0.4444 | 0.4444 | 0.4444 |
| 7,000 | 82.35 | 85 | 0.4804 | 0.4735 | 0.4709 | 0.4707 | 0.4706. | 0.4706 |
| 7,000 | 87.5 | 80 | 0.5114 | 0.5034 | 0.4995 | 0.4991 | 0.4990 | 0.4990 |
| 7,000 | 93.33 | 75 | 0.5465 | 0.5373 | 0.5342 | 0.5336 | 0.5334 | 0.5334 |

are shown in Fig. 4. Based on the observed relationships in these graphs, a mathematical formula was developed to represent the reference plastic buckling capacity ($PR_{pl}$) of concrete spherical shells for Ø = 20°–90°.

The formula, presented in Eq. (3), accounts for all the R/t and ($PR_{pl}$) values and was derived using the best-fit method:

$$PR_{pl} = 2.01 \cdot f_c' \cdot \frac{t}{R}. \quad (3)$$

In this equation, values for $f_c'$, *t*, and *R* should be substituted in MPa and mm, respectively.

As previously mentioned, a concrete compressive strength of 20 MPa was randomly selected for this study. Since plastic strength in concrete typically refers to its compressive strength, the material parameter $f_c'$ is incorporated into the formula.

Similarly, the elastic and plastic buckling capacities of EPSC shells are presented in Tables 5 and 6, respectively.

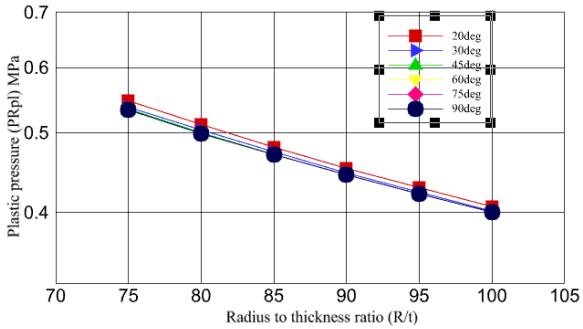


Fig. 4. Plastic buckling pressures for all Ø angles of the concrete shells

As described in Eqs. (1) and (2), to determine the modulus of elasticity of EPSC, the cube compressive strength (9.48 MPa) was converted to an equivalent cylinder strength (7.58 MPa), which was used throughout the analysis of EPSC shells.

Graphs of the plastic buckling capacities ($PR_{pl}$) versus *R*/*t* values for the 36 EPSC shells are shown in Fig. 5. Based on the relationship in the graphs and using the mathematical best-fit method, a formula similar to Eq. (3) was developed. This formula effectively represents the reference plastic buckling capacity of EPSC spherical shells and can significantly reduce the need for time-consuming software analyses. For instance, the ABAQUS result for a shell with *t* = 70 mm and *R*/*t* = 100 (third row of Table 6) yields a plastic buckling pressure value of 0.1523 MPa, which can be accurately reproduced using the developed formula.

The derived equation was compared to another formula proposed by Błażejewski (2022), given in Eq. (4):

$$PR_{pl} = 1.986 \cdot f_{yk} \cdot \frac{t}{R}. \quad (4)$$

Błażejewski's formula differs slightly from the one developed in this study. This discrepancy is primarily due to the difference in the shell geometry: Błażejewski considered thin spherical shells with *R*/*t* ratios between 300 and 1,000, whereas the current study focuses on moderately thick shells with R/t ratios ranging from 75 to 100. This is consistent with the understanding that shell thickness significantly influences structural plastic behavior (Li et al., 2021).

The plastic buckling capacities of EPSC shells, as summarized in Table 6, are significantly higher than the practical uniform external pressure acting on these shells (not exceeding 3 kN/m$^2$, accounting for a snow load of 1.5 kN/m$^2$ and the dead load from the self-weight of the EPSC shell).

Displacement analyses of the various shells revealed both symmetric and asymmetric deformation modes (Johnson, 1964; Van Isacker and Pittel, 2016; Verma et al., 2024). For example, the deformed shapes ºf concrete shells with Ø=75º, thickness 93.33 mm, and Ø=90º, thickness 87.5 mm are shown in Fig. 6(a, b), with displacements given in millimeters.

Similarly, Fig. 7 (a, b) illustrate the deformed shapes of EPSC shells with Ø=75º, thickness 93.33 mm, and Ø=90º, thickness 87.5 mm, respectively.

The displacement distribution shows that shells with Ø=75º exhibit symmetric deformation, while those with Ø=90º exhibit asymmetric deformation. This difference is primarily due to variations in shell height, which significantly affect collapse behavior (Gupta and Gupta,

Table 5. **Elastic Critical Buckling Pressures ($PR_{cr}$) of EPSC Shells**

| **Geometric Dimensions of the Shells** | | | **Critical Pressures for the Shells with Varying Half-Angle Ø (MPa)** | | | | | |
|---|---|---|---|---|---|---|---|---|
| *R* (mm) | *t* (mm) | *R*/*t* | 20º | 30º | 45º | 60º | 75º | 90º |
| 7,000 | 70 | 100 | 1.4226 | 1.3774 | 1.3466 | 1.3337 | 1.3254 | 1.3250 |
| 7,000 | 73.68 | 95 | 1.5751 | 1.5304 | 1.4937 | 1.4763 | 1.4669 | 1.4663 |
| 7,000 | 77.77 | 90 | 1.7565 | 1.7071 | 1.6647 | 1.6462 | 1.6361 | 1.6347 |
| 7,000 | 82.35 | 85 | 1.9756 | 1.9149 | 1.8692 | 1.8466 | 1.8330 | 1.8312 |
| 7,000 | 87.5 | 80 | 2.2438 | 2.1658 | 2.1132 | 2.0851 | 2.0714 | 2.0689 |
| 7,000 | 93.33 | 75 | 2.5777 | 2.4728 | 2.4064 | 2.3760 | 2.3554 | 2.3510 |

Table 6. **Plastic Buckling Pressures ($PR_{pl}$) (MPa) of EPSC Shells**

| **Geometric Dimensions of the Shells** | | | **Plastic Buckling Pressures for the Shells with Varying Ø** | | | | | |
|---|---|---|---|---|---|---|---|---|
| *R* (mm) | *t* (mm) | *R*/*t* | 20º | 30º | 45º | 60º | 75º | 90º |
| 7,000 | 70 | 100 | 0.1541 | 0.1523 | 0.1517 | 0.1516 | 0.1516 | 0.1516 |
| 7,000 | 73.68 | 95 | 0.1624 | 0.1604 | 0.1597 | 0.1595 | 0.1595 | 0.1595 |
| 7,000 | 77.77 | 90 | 0.1716 | 0.1693 | 0.1686 | 0.1684 | 0.1684 | 0.1684 |
| 7,000 | 82.35 | 85 | 0.1820 | 0.1794 | 0.1786 | 0.1784 | 0.1783 | 0.1783 |
| 7,000 | 87.5 | 80 | 0.1938 | 0.1907 | 0.1898 | 0.1896 | 0.1895 | 0.1895 |
| 7,000 | 93.33 | 75 | 0.2071 | 0.2036 | 0.2025 | 0.2023 | 0.2022 | 0.2021 |

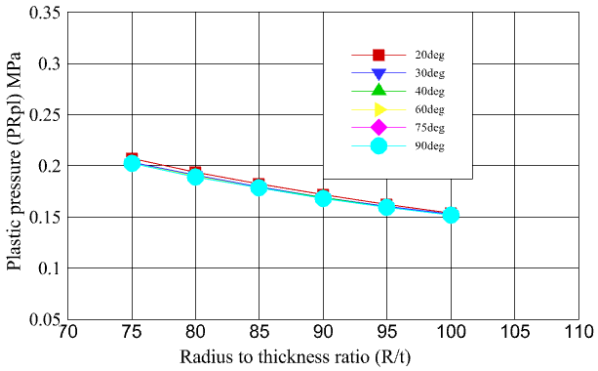


Fig. 5. Plastic buckling pressures for all Ø angles of EPSC shells

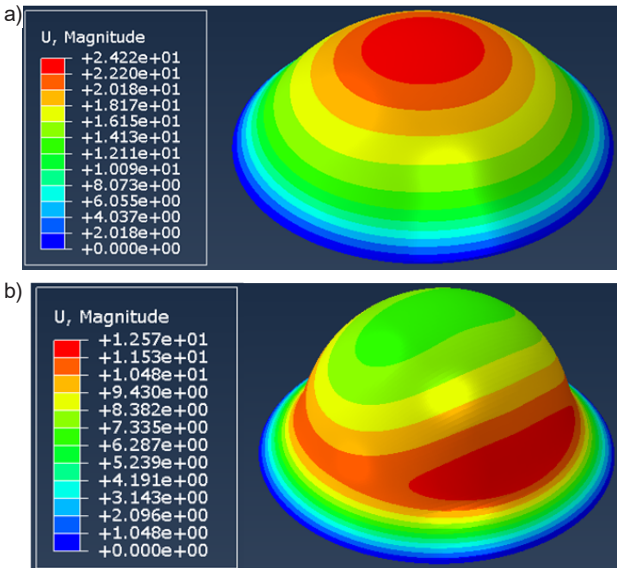


Fig. 6. Deformed shape of a concrete shell: a — with Ø=75º, thickness 93.33 mm; b — with Ø=90º, thickness 87.5 mm

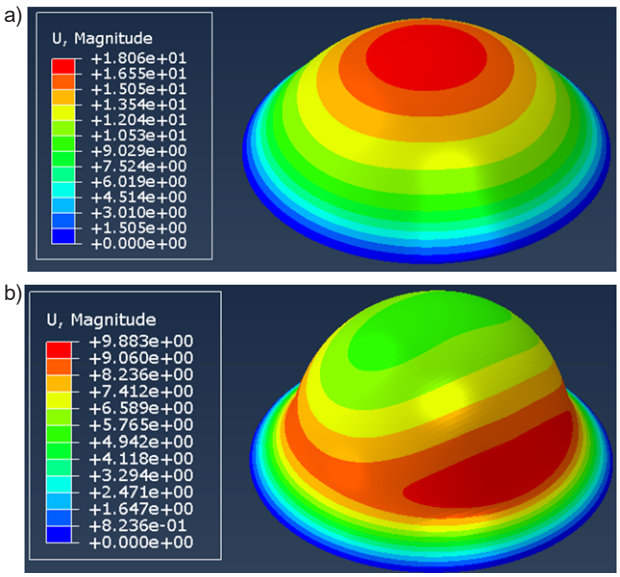


Fig. 7. Deformed shape of an EPSC shell: a — with Ø=75º, thickness 93.33 mm; b — with Ø=90º, thickness 87.5 mm

2009; Wang et al., 2016). Another contributing factor is the mode of energy dissipation. In the shells with Ø=75º, energy is dissipated through compression, while in the shells with Ø=90º, energy is dissipated through both bending and compression (Ruan et al., 2006).

From Figs. 6a and 7a, it is observed that the displacement of the EPSC shell (18 mm) with Ø=75º and thickness 93.33 mm is 1.34 times lower than that of the corresponding concrete shell (24.22 mm). This reduced displacement in EPSC shells is attributed to their lower self-weight.

Similarly, from Figs. 6b and 7b, the EPSC shell with Ø=90º and thickness 87.5 mm shows a displacement of 9.88 mm, which is 1.272 times lower than that of the corresponding concrete shell (12.57 mm).

**Conclusion**

This study investigated the plastic buckling capacity of expanded polystyrene concrete (EPSC) spherical shells in comparison to traditional concrete shells of identical geometry. Furthermore, analytical formulas for estimating the reference plastic buckling capacities of both concrete and EPSC spherical shells were developed. In the course of the study, the following conclusions were drawn.

Based on the experimental testing, the compressive strength, density, and elastic modulus of EPSC were found to be 9.48 MPa (7.58 MPa cylinder strength), 2074.17 kg/m$^3$, and 11.18 GPa, respectively. These values were used as input parameters for the numerical analyses to determine the elastic and plastic buckling capacities of EPSC spherical shells. The analyses showed that the plastic deformations of EPSC shells are 2.63 times lower than those of equivalent concrete shells. Moreover, the plastic buckling capacities of EPSC shells exceeded the actual external pressure loads. For instance, the displacements in EPSC shells shown in Fig. 7a (18.06 mm) and Fig. 7b (9.88 mm), for spans of 13.5 m and 14 m, respectively, are minimal. This illustrates the stiffness of EPSC shells and supports their potential use as an alternative to conventional concrete in shell structures.

The series of LBA and MNA analyses led to the development of an analytical formula for determining the plastic buckling capacities of concrete and EPSC spherical shells with half-opening angles Ø = 20º–90º. The formula depends on the shell radius, thickness, and compressive strength but is independent of the angle Ø. Using this formula can significantly reduce computational time for determining plastic buckling capacity.

As for future studies, it is recommended to investigate the stability of EPSC spherical shells with imperfections, including both geometric and material non-linearities.

**References**

Abood, A. H. (2020). Buckling analysis of large diameter concrete spherical shell domes. *Iraqi Journal for Mechanical and Material Engineering*. Special Issue (B), pp. 139–153.

ACI Committee (2019). *Building code requirements for structural concrete* (ACI 318-19). Farmington Hills, MI: American Concrete Institute, 624 p.

Aghaee, K. and Foroughi, M. (2013). Mechanical properties of lightweight concrete partition with a core of textile waste. *Advances in Civil Engineering*, Vol. 2013, 482310. DOI: 10.1155/2013/482310.

Akçaözoğlu, S., Atiş, C. D., and Akçaözoğlu, K. (2010). An investigation on the use of shredded waste PET bottles as aggregate in lightweight concrete. *Waste Management*, Vol. 30, Issue 2, pp. 285–290. DOI: 10.1016/j.wasman.2009.09.033.

Akter, T., Ferdous Wahid, M., and Siddique, A. B. (2017). Strength variation of concrete between cylindrical and cubical specimen due to various proportion of ingredients. *Sonargaon University Journal*, Vol. 2, No. 2, pp. 56–64.

Błażejewski, P. (2022). Development of a procedure for the determination of the buckling resistance of steel spherical shells according to EC 1993-1-6. *Materials*, Vol. 15, Issue 1, 25. DOI: 10.3390/ma15010025.

Budiansky, B. and Hutchinson, J. W. (1966). A survey of some buckling problems. *AIAA Journal*, Vol. 4, No. 9, pp. 1505–1510. DOI: 10.2514/3.3727.

Bushnell, D. (1982). Plastic buckling of various shells. *Journal of Pressure Vessel Technology*, Vol. 104, Issue 2, pp. 51–72. DOI: 10.1115/1.3264190.

Damir, H. Y., Rynkovskaya, M., and Sereke, I. A. (2024). Comparative buckling analysis of concrete and expanded polystyrene dome shells. *Architecture and Engineering*, Vol. 9, No. 1, pp. 71–78. DOI: 10.23968/2500-0055-2024-9-1-71-78.

Do, V.-D., Le Grognec, P., and Rohart, P. (2023). Closed-form solutions for the elastic-plastic buckling design of shell structures under external pressure. *European Journal of Mechanics - A/Solids*, Vol. 98, 104861. DOI: 10.1016/j.euromechsol.2022.104861.

European Committee for Standardization (2007). *EN 1993-1-6. Eurocode 3 - Design of steel structures - Part 1-6: Strength and stability of shell structures*. [online] Available at: https://www.phd.eng.br/wp-content/uploads/2015/12/en.1993.1.6.2007.pdf [Date accessed: November 1, 2024].

Gupta, P. K. and Gupta, N. K. (2009). A study of axial compression of metallic hemispherical domes. *Journal of Materials Processing Technology*, Vol. 209, Issue 4, pp. 2175–2179. DOI: 10.1016/j.jmatprotec.2008.05.004.

Hutchinson, J. W. (2016). Buckling of spherical shells revisited. *Proceedings of the Royal Society A. Mathematical, Physical and Engineering Sciences*, Vol. 472, Issue 2195, 20160577. DOI: 10.1098/rspa.2016.0577.

Johnson, D. E. (1964). Nonsymmetric bending deformation of spherical shells. *Journal of Applied Mechanics*, Vol. 31. Issue 2, pp. 344–345. DOI: 10.1115/1.3629614.

Li, J., Ren, H., and Ning, J. (2021). Deformation and failure of thin spherical shells under dynamic impact loading: experiment and analytical model. *Thin-Walled Structures*, Vol. 161, 107403. DOI: 10.1016/j.tws.2020.107403.

Liu, N. and Chen, B. (2014). Experimental study of the influence of EPS particle size on the mechanical properties of EPS lightweight concrete. *Construction and Building Materials*, Vol. 68, pp. 227–232. DOI: 10.1016/j.conbuildmat.2014.06.062.

Liu, T., Chen, Y., Hutchinson, J. W., and Jin, L. (2022). Buckling of viscoelastic spherical shells. *Journal of the Mechanics and Physics of Solids*, Vol. 169, 105084. DOI: 10.1016/j.jmps.2022.105084.

Maghfouri, M., Shafigh, P., Alimohammadi, V., Doroudi, Y., and Aslam, M. (2020). Appropriate drying shrinkage prediction models for lightweight concrete containing coarse agro-waste aggregate. *Journal of Building Engineering*, Vol. 29, 101148. DOI: 10.1016/j.jobe.2019.101148.

Muc, A., Kubis, S., Bratek, Ł., and Muc-Wierzgoń, M. (2022). Higher order theories for the buckling and post-buckling studies of shallow spherical shells made of functionally graded materials. *Composite Structures*, Vol. 295, 115851. DOI: 10.1016/j.compstruct.2022.115851.

Neville, A. M. (2012). *Properties of concrete*. 5th ed. Harlow, England: Prentice Hall, 846 p.

Rotter, J. M. and Schmidt, H. (2013). *Buckling of steel shells: European design recommendations*. 5th ed. Brussels [online] Available at https://lib.ugent.be/catalog/rug01:002206396#reference-details [Date accessed: November 15, 2024].

Ruan, H. H., Gao, Z. Y., and Yu, T. X. (2006). Crushing of thin-walled spheres and sphere arrays. *International Journal of Mechanical Sciences*, Vol. 48, Issue 2, pp. 117–133. DOI: 10.1016/j.ijmecsci.2005.08.006.

Saradhi Babu, D., Ganesh Babu, K., and Wee, T. H. (2005). Properties of lightweight expanded polystyrene aggregate concretes containing fly ash. *Cement and Concrete Research*, Vol. 35, Issue 6, pp. 1218–1223. DOI: 10.1016/j.cemconres.2004.11.015.

Sato, M., Wadee, M. A., Iiboshi, K., Sekizawa, T., and Shima, H. (2012). Buckling patterns of complete spherical shells filled with an elastic medium under external pressure. *International Journal of Mechanical Sciences*, Vol. 59, Issue 1, pp. 22–30. DOI: 10.1016/j.ijmecsci.2012.02.001.

Srinivas, K., Akula, K. R., and Mahesh, V. (2021). Experimental investigation on lightweight concrete by replacing the coarse aggregate with coconut shell and expanded polystyene beads and using polypropylene fiber. *Materials Today: Proceedings*, Vol. 46, Part 1, pp. 838–842. DOI: 10.1016/jmatpr.2020.12.834.

Sri Ravindrarajah, R. and Tuck, A. J. (1994). Properties of hardened concrete containing treated expanded polystyrene beads. *Cement and Concrete Composites*, Vol. 16, Issue 4, pp. 273–277. DOI: 10.1016/0958-9465(94)90039-6.

Teo, D. C. L., Mannan, M. A., and Kurian, V. J. (2006). Structural concrete using oil palm shell (OPS) as lightweight aggregate. *Turkish Journal of Engineering and Environmental Sciences*, Vol. 30, No. 4, pp. 251–257.

Van Isacker, P. and Pittel, S. (2016). Symmetries and deformations in the spherical shell model. *Physica Scripta*, Vol. 91, No. 2. DOI: 10.1088/0031-8949/91/2/023009.

Gaurav, V., Gagandeep, I., and Hargun, K. S. (2024). Deformation analysis of spherical shell by using generalized Hooke's law. *Structural Integrity and Life*, Vol. 24, No. 1, pp. 61–64. DOI: 10.69644/ivk-2024-01-0061.

Wang, S., Li, S., He, J., and Zhao, Y. (2016). Asymmetric postbuckling behavior of hemispherical shell structure under axial compression. *Journal of Engineering Materials and Technology*, Vol. 138, Issue 1, 011005. DOI: 10.1115/1.4031960.

Wang, J., Li, Z. L., and Yu, W. (2019). Structural similitude for the geometric nonlinear buckling of stiffened orthotropic shallow spherical shells by energy approach. *Thin-Walled Structures*, Vol. 138. pp. 430–457. DOI: 10.1016/j.tws.2018.02.006.

Yasin, E., Ergul, Y., and Pathegama, G. R. (2016). Obtaining lightweight concrete using colemanite waste and acidic pumice. *Physicochemical Problems of Mineral Processing*, Vol. 52, No. 1, pp. 35–43. DOI: 10.5277/ppmp160103.

Zhang, J., Zhang, M., Tang, W., Wang, W., and Wang, M. (2017). Buckling of spherical shells subjected to external pressure: a comparison of experimental and theoretical data. *Thin-Walled Structures*, Vol. 111, pp. 58–64. DOI: 10.1016/j.tws.2016.11.012.

Zia, P., Ahmad, S., and Leming, M. (1997). *High-performance concretes, a state-of-art report (1989-1994)*. [online] Available at: https://rosap.ntl.bts.gov/view/dot/56419 [Date accessed: November 15, 2024].

Zoelly, R. (1915). *Ueber ein Knickungsproblem an der Kugelschale*. PhD Thesis in Engineering. DOI: 10.3929/ethz-a-000091951.

# АНАЛИЗ ПЛАСТИЧЕСКОЙ ПОТЕРИ УСТОЙЧИВОСТИ СФЕРИЧЕСКИХ ОБОЛОЧЕК ИЗ ОБЫЧНОГО БЕТОНА И ПОЛИСТИРОЛБЕТОНА

Иссаиас Андай Сереке*, Марина Игоревна Рынковская, Хабте Йоханнес Дамир

Российский университет дружбы народов им. Патриса Лумумбы, Москва, Россия

*E-mail: issaiasanday@gmail.com

**Аннотация**

**Введение**: Собственный вес бетона представляет собой основную причину увеличения сечений и постоянной нагрузки в конструкциях. Данная проблема может быть частично решена за счет использования легкого бетона. Полистиролбетон по весу легче обычного бетона, но до настоящего момента не применялся в оболочках. **Цель исследования** — проанализировать и сравнить пластическую устойчивость куполов из обычного бетона и полистиролбетона, а также вывести аналитическую формулу для определения пластической устойчивости сферических оболочек из этих материалов. **Методика** включает экспериментальное исследование кубических образцов для оценки свойств полистиролбетона. По результатам испытаний прочность на сжатие, плотность и модуль упругости полистиролбетона составили соответственно 9,48 МПа, 2074,17 кг/м$^3$ и 11,18 ГПа. Затем с помощью программного комплекса ABAQUS были проведены линейный анализ потери устойчивости и нелинейный анализ материалов для определения упругой и пластической устойчивости 36 сферических оболочек из бетона и 36 сферических оболочек из полистиролбетона. На основе полученных данных выведена аналитическая формула для оценки пластической устойчивости как оболочек из бетона, так и оболочек из полистиролбетона. **Результаты** показывают, что пластическая устойчивость оболочек из полистиролбетона значительно превышает практически действующие равномерные внешние нагрузки. Однако при этом она ниже, чем у аналогичных бетонных оболочек. Тем не менее оболочки из полистиролбетона демонстрируют меньшие пластические деформации и смещения по сравнению с бетонными оболочками, что указывает на достаточную жесткость и подтверждает возможность использования полистиролбетона в сферических оболочечных конструкциях. Предложенная формула может применяться для определения базовой пластической устойчивости сферических оболочек из бетона и полистиролбетона.

**Ключевые слова:** потеря устойчивости; давление; бетон; смещение; сферические оболочки.